Journal of The Electrochemical Society, **158** (5) K117-K122 (2011)
0013-4651/2011/158(5)/K117/6/$28.00 © The Electrochemical Society

Characterization of Poly(brilliant cresyl blue)-Multiwall Carbon Nanotube Composite Film and Its Application in Electrocatalysis of Vitamin B_9 Reduction

Yogeswaran Umasankar,[*] Tzu-Wei Ting, and Shen-Ming Chen[,z]**

Department of Chemical Engineering and Biotechnology, National Taipei University of Technology, No. 1, Section 3, Taipei 106, Taiwan

Electrochemically active composite film which contains multi-walled carbon nanotubes (MWCNTs) incorporated with poly(brilliant cresyl blue) (PBCB) has been prepared on glassy carbon electrode (GCE) and indium tin oxide (ITO) electrode by potentiodynamic method. The presence of MWCNTs in the composite film (MWCNTs-PBCB) enhances the surface coverage concentration (Γ) of PBCB by 0.25 nmol cm^{-2} μg^{-1}. The surface morphology of various films deposited on ITO has been studied using scanning electron microscopy and atomic force microscopy, which reveals that MWCNTs incorporated with PBCB. The MWCNTs-PBCB composite film exhibits promising enhanced electrocatalytic activity towards the biochemical compound vitamin B_9 (folic acid). The electrocatalytic response of folic acid at PBCB, MWCNTs and MWCNTs-PBCB composite films have been studied using cyclic voltammetry (CV) and differential pulse voltammetry (DPV). The sensitivity of MWCNTs-PBCB film towards folic acid (177 $\mu A\ mM^{-1}\ cm^{-2}$) is higher than the values obtained for PBCB (0.75 $\mu A\ mM^{-1}\ cm^{-2}$) and MWCNT films (148 $\mu A\ mM^{-1}\ cm^{-2}$). Similarly, the limit of detection of folic acid at MWCNTs-PBCB film (76 μM) is lower than the other two films. Further, the DPV and selectivity studies reveal that the MWCNTs-PBCB film is efficient for folic acid determination in real sample.
 [DOI: 10.1149/1.3556098]

Manuscript submitted November 8, 2010; revised manuscript received January 17, 2011. Published March 9, 2011.

Vitamin B_9 (folic acid) is a water-soluble vitamin, its deficiency in humans causes various chronic diseases such as leucopoenia, gigantocytic anemia and even heart attack especially during carcinogenic processes.[1,2] Due to its crucial role in biological system several traditional determination methods were developed, such as fluorescence, phosphorescence, chromatography, spectrophotometry, electroanalysis, etc.[3–5] Among these methods, electrochemical determination of folic acid showed promising results in the past decade.[1,6,7] However electrochemical analysis using unmodified electrodes has limitations, for example glassy carbon electrode (GCE) has pronounced fouling effect, poor selectivity and reproducibility. To overcome these limitations and to enhance the electrocatalysis reaction of folic acid, electrodes were modified using catalysts such as polymer-immobilized sol-gels,[1] functionalized thiadiazole[6] and phosphomolybdic-polypyrrole.[7]

Among the electrode modification techniques electropolymerization is a simple but powerful method in targeting selective modification of different type electrodes with desired matrices. The electroactive polymers and carbon nanotube (CNT) matrices have received considerable attraction in recent years. Numerous conjugated polymers were electrochemically synthesized for the fabrication of chemical and biochemical sensor devices.[8–11] These conjugated polymers exhibits enhancement in the electrocatalytic activity towards the oxidation or reduction of several chemical and biochemical compounds,[12] where some of the functional groups in polymer act as catalyst.[13–15] In this article the term "enhanced electrocatalytic activity" define both "increase in peak current" and "lower overpotential."[16] Similar to conjugated polymers, the wide applications of CNT matrices in the detection of chemical and biochemical compounds have also been reported in the literature.[17–20]

Even though the electrocatalytic activity of conjugated polymers and CNT matrices individually show good results, some properties like mechanical stability, sensitivity for different techniques, and electrocatalysis for multiple compounds are found to be poor. To overcome these drawbacks new studies were developed in the past decade for the preparation of composite films composed of both CNTs and conjugated polymers. The rolled-up graphene sheets of carbon exhibit π-conjugative structure with highly hydrophobic surface. This unique property of the CNTs allows them to interact with organic aromatic compounds through π-π electronic and hydrophobic interactions to form new structures.[21,22] There were past attempts in the preparation of composite and sandwiched films made of polymer adsorbed on CNT matrices, and they were used for electrocatalytic studies.[23] The sandwiched films were also used in the designing of nanodevices with the help of non-covalent adsorption, electrodeposition, etc.[24,25]

Among conjugated polymers a group of them representing azines have wide use as redox indicators and mediators in bioelectrochemistry.[26] The electropolymerization of azine group monomers were usually performed by anodic oxidation in acidic medium.[27,28] In azine dyes brilliant cresyl blue (BCB) is a cationic quinine-imide dye with a planar rigid structure with promising properties as a redox catalyst with features like fast rate of charge transfer and ion transport.[29–31] Previous studies reported poly(brilliant cresyl blue) (PBCB) can be synthesized by electrochemical polymerization of BCB. These studies reported also the growth mechanism of PBCB along with the electrochemical studies.[30,31] In this article we report a composite film (MWCNTs-PBCB) made of multi-walled carbon nanotubes (MWCNTs) incorporated with PBCB. MWCNTs-PBCB composite film's characterization, enhancement in functional properties, peak current and electrocatalytic activity have also been reported along with its application in the determination of folic acid. The MWCNTs-PBCB composite film formation processing involves the modification of electrode with uniformly well dispersed MWCNTs, and which is then modified with PBCB.

Experimental

Materials.—BCB, MWCNTs (OD = 7–15 nm, ID = 3–6 nm, and length = 0.5–200 μm) and folic acid obtained from Aldrich and Sigma-Aldrich were used as received. All other chemicals used were of analytical grade. The preparation of aqueous solution was done with twice distilled deionized water. Solutions were deoxygenated by purging with pre-purified nitrogen gas. Phosphate buffer solution (PBS) *p*H 7.0 was prepared from 0.1 M Na_2HPO_4 and 0.1 M NaH_2PO_4 aqueous solutions.

Apparatus.—Cyclic voltammetry (CV) and differential pulse voltammetry (DPV) were performed using analytical system models CHI-1205 and CHI-750 potentiostats, respectively. A conventional three-electrode cell assembly consisting of an Ag/AgCl reference electrode and a Pt wire counter electrode were used for electrochemical measurements. The working electrode was GCE modified either with PBCB, MWCNTs or MWCNTs-PBCB composite films. In all the experimental results potential is reported versus Ag/AgCl

[*] Electrochemical Society Student Member.
[**] Electrochemical Society Active Member.
[z] E-mail: smchen78@ms15.hinet.net

reference electrode. The morphological characterizations of the various films were examined by means of scanning electron microscopy (SEM) (Hitachi S-3000H) and atomic force microscopy (AFM) (Being Nano-Instruments CSPM4000). All the measurements were carried out at 25° C ± 2.

Preparation of MWCNTs-PBCB composite film modified electrodes.—The important challenge in the preparation of MWCNTs solution for electrode modification was the difficulty in dispersing it in to a homogeneous solution. Generally, the dispersion of CNTs were carried out by physical (milling) and chemical methods (covalent and noncovalent functionalization). Briefly, by following previously reported method[32,33] 50 mg of MWCNTs were heated in a crucible at 350°C for 2 h to remove the amorphous carbon and catalyst impurities, and then cooled to room temperature. This heat treated MWCNTs were ultrasonicated for 4 h in 20 mL conc. HCl to remove other impurities, and washed several times with water and then dried at 100°C in air oven. The repeated washing was carried out by a suction filter setup where 50 mL of water was added each time on the MWCNTs and rinsed and then filtered. The above step was carried out ten times before drying MWCNTs. These purified and dried MWCNTs were acid treated using sulfuric acid and nitric acid (3:1) by 6 h ultrasonication at room temperature, and then washed several times with water until the *p*H of supernatant was neutral. Washing in water was carried out by the same method mentioned before, and *p*H of the filtrate was measured using *p*H paper. To measure the exact *p*H, MWCNT was dispersed in water and the supernatant was measured using a standard *p*H meter. The washing steps were repeated until the *p*H of supernatant was neutral. These acid treated MWCNTs have been dried overnight at 60°C. Finally the uniform dispersion of MWCNTs was obtained by 6 h ultrasonication of 10 mg acid treated MWCNTs in 10 mL water.

Before starting each experiment GCEs were polished by BAS polishing kit with 0.05 μm alumina slurry and they were rinsed and then ultrasonicated in double distilled deionized water. The GCEs studied were uniformly coated with 50 µg cm^{-2} of MWCNTs and dried at room temperature. The coating of MWCNTs was carried out by pouring known amount of MWCNT dispersion on GCE surface using micro-syringe and then dried. Then the BCB was electropolymerized on MWCNTs modified GCE. The electrolyte used for BCB electropolymerization was PBS with 1 mM BCB. The electropolymerization was performed by consecutive cyclic voltammograms over a suitable potential range of –0.6 to 1.2 V with scan rate = 50 mV s^{-1}. Then the modified MWCNTs–PBCB electrode was carefully washed with double distilled deionized water.

Results and Discussion

Electropolymerization of BCB at various electrodes and their characterizations.—The electropolymerization of BCB using electrochemical oxidation on unmodified and MWCNTs modified GCEs have been performed for the preparation and comparative studies of PBCB and MWCNTs-PBCB composite films. In electropolymerization cyclic voltammograms, on subsequent cycles the redox peaks correspond to PBCB have found growing in both bare and MWCNTs modified electrodes (figure not shown). This result indicates that during the cycle deposition of PBCB takes place on the bare and MWCNTs modified GCE surface. The possible adsorption site of PBCB at MWCNT is given in Fig. 1, where the minimum free energy is –4.3 kcal mol^{-1}. The docking of BCB trimer on acid treated MWCNTs has been carried out using Lamarckian genetic algorithm.[34,35] The simulation conditions such as population size (50), maximum generations (3000), crossover rate (0.8), mutation rate (0.2), elitism (5), local search rate (0.06) and local search maximum steps (100) were kept constant and the area around the binding site was varied to obtain lowest free energy possible. The plot of binding site area versus free energy in Fig. 1 shows the lowest free energy can be obtained if the binding site area around the MWCNT

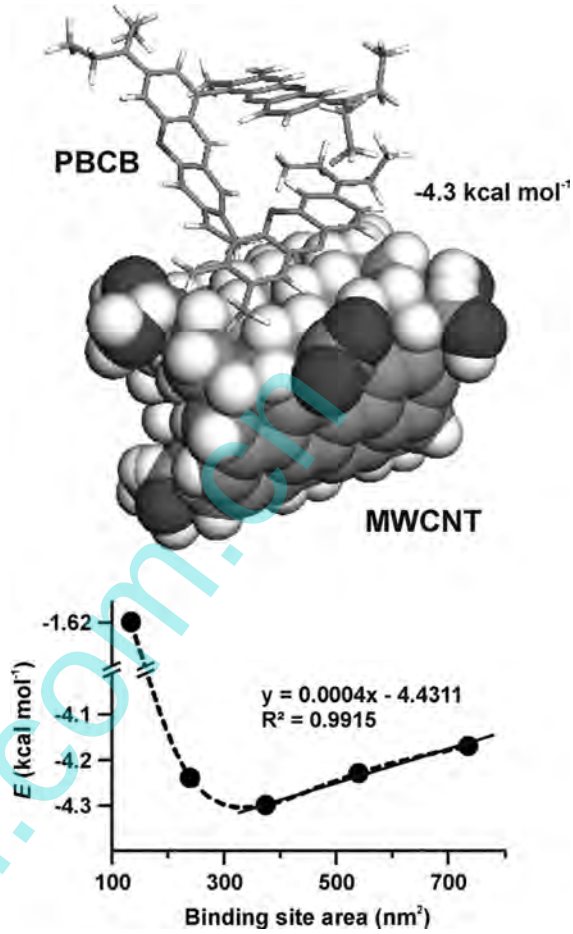

Figure 1. Possible adsorption site of PBCB at MWCNT given by Lamarckian genetic algorithm. The plot shows the change in free energy with respect to binding site area.

is 375 nm^2. The same plot shows the free energy reduces while the binding site area increases until 375 nm^2, however the increase in binding site area after 375 nm^2 increases the free energy at the rate of 0.4 cal mol^{-1} nm^{-2}.

The prepared films (PBCB, MWCNTs-PBCB) along with only MWCNTs have been characterized using various electrochemical techniques in PBS. Before transferring the films in to aqueous solution for other electrochemical characterizations, the prepared films have been washed carefully in deionized water to remove the loosely attached non-polymerized BCB monomer present on the modified GCE. Figure 2 shows the reversible redox couples of PBCB at bare and MWCNTs modified GCEs, and only MWCNTs (without PBCB). The corresponding cyclic voltammograms were measured at 50 mV s^{-1} scan rate in the potential range of 0.6 to –0.6 V. Among these three films the E^0 of redox couples for PBCB are at –107 and –368.5 mV, and for MWCNT-PBCB composite film they are at 148.5 and –126 mV. The PBCB electrochemical signal at more negative redox couple corresponds to the residual BCB and the more positive redox couple represents the bridged nitrogen in PBCB.[29] This property of PBCB is similar to the previously reported azine dye polymer's property.[8,36,37] Similarly the redox reaction of MWCNTs is represented by $E^{0'} = 108$ mV. This redox reaction at MWCNTs is due to the carboxyl groups on the surface of MWCNTs.[29,38] The anodic potential (Epa), cathodic potential (Epc) and cathodic current (Ipc) values of PBCB at various film modified electrodes are given in Table I. Interestingly the values in Table I reveals MWCNT modified GCE has higher polymerizing current for PBCB than at unmodified GCE. These above

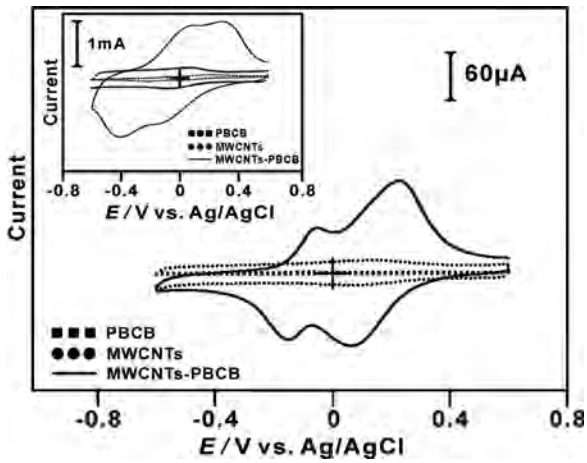

Figure 2. Cyclic voltammograms of GCE modified from PBCB, MWCNTs and MWCNTs-PBCB films in *p*H 7.0 PBS solution, potential between 0.6 and –0.6 V with scan rate at 50 mV s^{-1}. Inset is the cyclic voltammograms of ITO modified from PBCB, MWCNTs and MWCNTs-PBCB films at similar conditions.

results represent more deposition of PBCB on MWCNT modified GCE than on bare GCE.

The increase in deposition of PBCB in presence of MWCNTs are evident with the active surface coverage concentration (Γ) given in Table I, where Γ of PBCB enhanced at MWCNTs film modified GCE when comparing bare GCE. The Γ has been calculated using the equation $\Gamma = Q/nFA$, where Q is charge involved, n is number of electrons, F is Faraday constant and A is the area of electrode. The calculated values from the same table show that MWCNTs enhances Γ of PBCB by 0.25 nmol cm^{-2} μg^{-1}. In these Γ calculations the number of electrons involved in PBCB redox reactions is assumed as two. The comparison of PBCB, MWCNTs and MWCNTs-PBCB films on indium tin oxide (ITO) electrodes are given in Fig. 2 inset. In the ITO experiments too MWCNTs modified electrode show higher polymerizing current for PBCB than at unmodified electrode, which are consistent with the Ipc and Γ values given in Table I.

SEM and AFM studies of PBCB, MWCNTs, and MWCNTs-PBCB composite films.—Three different films PBCB, MWCNTs and MWCNTs-PBCB were prepared on indium tin oxide electrodes with similar conditions and similar potential as that of GCE, and were characterized using SEM and AFM. The top views of nanostructures in Fig. 3a on the ITO electrode surface shows the presence of clusters of PBCB. The MWCNTs film in Fig. 3b shows uniform formation of film from a good dispersion of MWCNTs solution. The MWCNTs-PBCB composite film in Fig. 3c shows that clusters of PBCB formed over MWCNTs film modified ITO electrode. Further, in Fig. 3c the amount of PBCB is higher than the

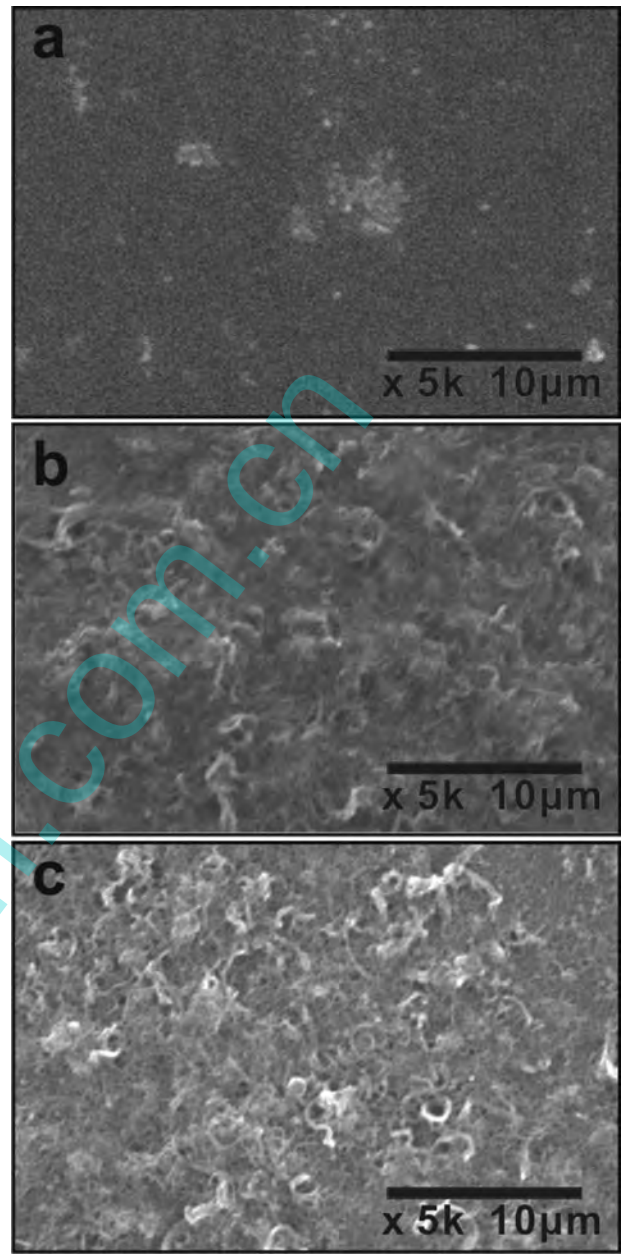

Figure 3. SEM images of (a) PBCB, (b) MWCNTs, and (c) MWCNTs-PBCB films.

amount formed on bare electrode in Fig. 3a, which could be explained as the increase in deposition of PBCB in presence of MWCNTs. The higher concentration of PBCB deposited on

Table I. Epa, Epc, Ipc values of redox reactions of PBCB and surface coverage concentration (Γ) of PBCB at various modified electrodes present in PBS.

Modified Electrodes					
Electrodes	Films	Epa (mV)	Epc (mV)	Ipc (μA)	Γ (nmol cm^{-2})
GCE	PBCB[a]	–75, –332	–139, –405	–0.6124, –0.08	0.07
	MWCNTs	146	70	–6.151	–
	PBCB[b]	228, –51	69, –150	–75.55, –17.21	12.7
ITO	PBCB[a]	214, –87	32, –214	–44.02, –21.37	0.71
	MWCNTs	66	–77	–123.2	–
	PBCB[b]	287.2, 94.1	–121, –401	–679.3, –232.9	31.4

[a]PBCB electropolymerized on bare electrode.
[b]PBCB electropolymerized on MWCNTs modified electrode.

MWCNTs modified ITO electrode when comparing bare electrode is consistent with the Γ values shown in Table I. The magnified view of the same three films in AFM Figs. 4a–4c reveals also the morphological difference. In these results instead of clusters Fig. 4a shows the beads of PBCB deposited over ITO surface, and uneven surface of MWCNTs and MWCNTs-PBCB in Fig. 4a and 4b respectively. Further, the thicknesses of PBCB, MWCNTs and MWCNTs-PBCB obtained using AFM results are 231, 869, and 1700 nm respectively. The values show MWCNTs-PBCB composite film has higher thickness than other two films. These SEM and AFM results reveal the coexistence of MWCNTs and PBCB as a composite film.

Electrochemical and stability studies of MWCNTs-PBCB composite film.—The cyclic voltammograms of MWCNTs-PBCB composite film on GCE in PBS at different scan rate show that the anodic and cathodic peak current of composite film's redox couple increases linearly with the increase of scan rate. The ratio of Ipa/Ipc (Ipa is anodic current) for MWCNTs-PBCB film demonstrates that the redox process was not controlled by diffusion until 460 mV s^{-1}. However, the ΔEp of each scan rate reveals that the peak separation of MWCNTs-PBCB film's redox couple increases as the scan rate increase (figure not shown). The effect of *p*H on MWCNTs-PBCB composite film has also been studied (figure not shown). Where, it revealed the cyclic voltammograms of MWCNTs-PBCB on GCE obtained in various *p*H aqueous buffer solutions without the presence of BCB. The MWCNTs-PBCB composite film preparation was carried out in PBS as mentioned in experimental section, and then washed with deionized water before transferring it in to various *p*H solutions. The results show that the film is stable in the *p*H range between 1 and 11. The values of Epa and Epc depends on the *p*H value of buffer solution. The response from the plot of MWCNTs-PBCB's formal potential versus *p*H shows a slope of 48 mV pH^{-1}, which is close to that given by Nernstian equation for equal number of electrons and protons transfer.

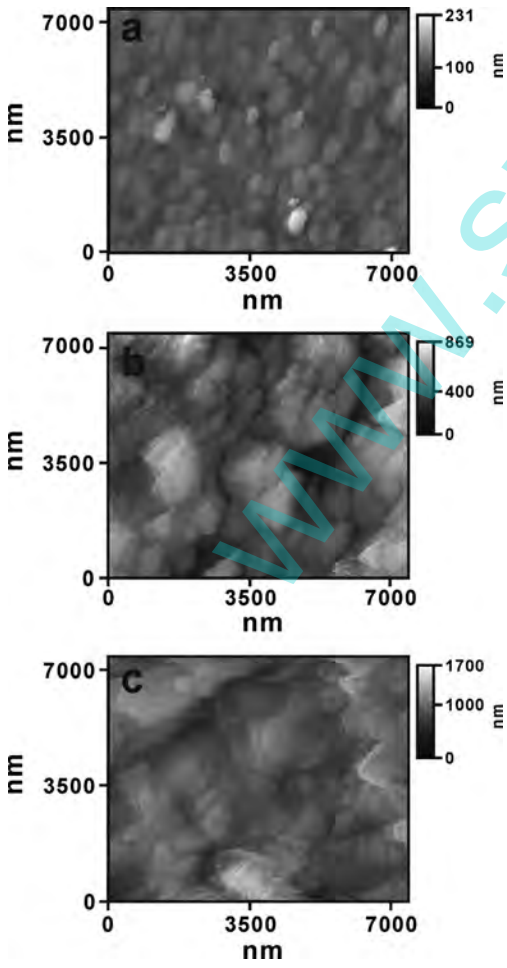

Figure 4. AFM images of (a) PBCB, (b) MWCNTs, and (c) MWCNTs-PBCB films.

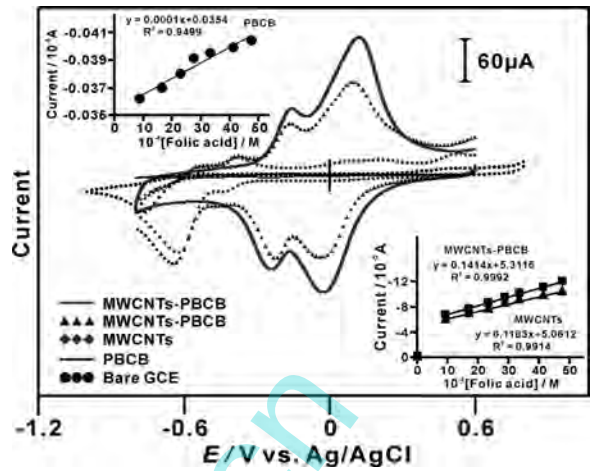

Figure 5. Cyclic voltammograms of folic acid (4.7 mM) at bare GCE, PBCB, MWCNTs, and MWCNTs-PBCB composite film modified GCEs using PBS at 50 mV s^{-1}, where MWCNTs-PBCB composite film is shown with both absence (continuous line in cyclic voltammogram) and presence (triangles in cyclic voltammogram) of 4.7 mM folic acid. The insets are the plots of peak current (Ipc) vs concentration of folic acid at PBCB (top), MWCNTs and MWCNTs-PBCB (bottom) respectively.

The enhancement in stability of PBCB in the presence of MWCNTs has been studied, and the percentage of degradation of MWCNTs-PBCB and PBCB has been calculated using an equation given in previous literature.[39] The experiment was conducted with the successive 180 min cycling (scan rate 50 mV s^{-1}) applied over a potential range of –0.6 to 0.6 V on MWCNTs-PBCB and PBCB in PBS (figure not shown). The cyclic voltammograms have been recorded at the interval of 30 min each, from which the values of Ipc were noted and plotted against time. From the results it is clear that after 90 min the response of MWCNTs-PBCB and PBCB becomes constant with time and cycling, indicating both are stable films. However, the amount of degradation after 180 min cycling for MWCNTs-PBCB and PBCB are 18 and 21% respectively. From this above result the percentage of decrease in degradation of PBCB in presence of MWCNTs is about 3% for 180 min cycling. Similar enhancements in CNTs-polymer composite properties when comparing CNT or polymer alone were already reported in the literature.[40]

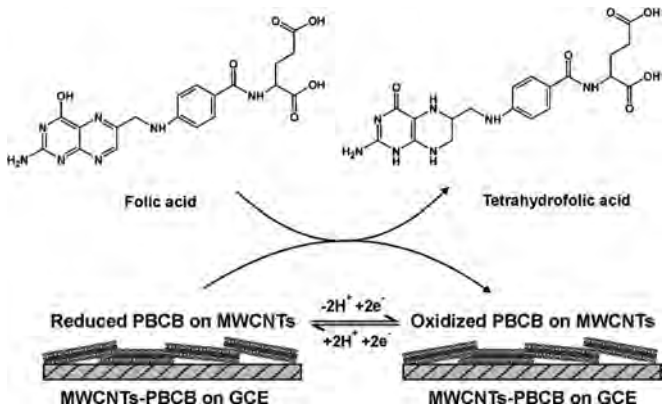

Figure 6. Electrochemical reduction of folic acid at the MWCNTs-PBCB composite modified electrode.

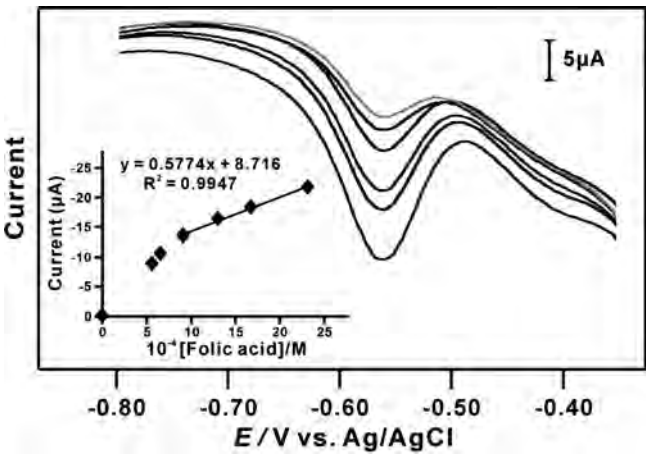

Figure 7. Differential pulse voltammograms of folic acid (0.56–2.31 mM) at MWCNTs-PBCB composite film modified GCE using PBS. Inset represents the plot of peak current (Ipc) vs concentration of folic acid.

Electroanalytical response of folic acid at MWCNTs-PBCB composite film.—The MWCNTs-PBCB composite film has been synthesized on GCE at similar conditions as given in experimental section. Then the MWCNTs-PBCB composite film GCE has been washed carefully in deionized water and transferred to PBS for the electrocatalysis of folic acid. All the cyclic voltammograms have been recorded at the constant time interval of 1 min with N_2 purging before the start of each experiment. Figure 5 shows the electrocatalytic reduction of folic acid (4.74 mM) at various film modified and unmodified GCEs with scan rate = 50 mV s^{-1}. The various film modified GCEs tested are PBCB, MWCNTs and MWCNTs-PBCB composite, where the MWCNTs-PBCB composite film is shown with highest concentration (4.74 mM) and in the absence of folic acid. The schematic representation of folic acid electrochemical reduction at MWCNTs-PBCB composite film is given in Fig. 6. The cyclic voltammogram for MWCNTs-PBCB composite film exhibits reversible redox couples in the absence of folic acid, and upon addition of folic acid a new growth in the reduction peak of folic acid appears at Epc = –638 mV. Similarly, the reduction peak of folic acid for bare GCE, PBCB, and MWCNTs films appears at Epc = –767, –667, and –626 mV, respectively. In these above electrocatalysis experiments, an increase in concentration (0.91–4.74 mM) of folic acid simultaneously produces a linear increase in reduction peak current of folic acid with good film stability for all the three films. However, there is no increase in the peak current at bare GCE.

It is obvious that the MWCNTs-PBCB composite film shows higher electrocatalytic activity for folic acid when comparing other two films. In detail the enhanced electrocatalytic activity of MWCNTs-PBCB composite film can be explained in terms of both lower in overpotential and higher peak current of folic acid than at PBCB and bare GCE; and higher peak current than at MWCNTs. Where, the increase in peak current and decrease in overpotential; both are considered as the electrocatalytic activity.[16] The Ipc of folic acid (4.47 mM) at bare GCE is –50.8 μA, PBCB is –0.4 μA, MWCNTs is –105 μA, and MWCNTs–PBCB is –120 μA. These above Epc and Ipc values shows that the enhancement in electrocatalytic activity at MWCNTs-PBCB composite film is due to presence of both MWCNTs and PBCB, where the cathodic peak potential is lowered by MWCNTs, and the peak current is enhanced by both MWCNTs and PBCB. From the slopes of linear calibration curves (Fig. 5 insets) the sensitivity of PBCB, MWCNTs and MWCNTs-PBCB composite film modified GCEs have been calculated and they are 0.75, 148, and 177 μA mM^{-1} cm^{-2} respectively, and the correlation coefficients are 0.9499, 0.9914, and 0.9992 respectively. It is obvious that the sensitivity of MWCNTs-PBCB composite film is higher for folic acid when comparing PBCB and MWCNTs films. From the same results, folic acid's limit of detection (LOD) at PBCB, MWCNTs and MWCNTs-PBCB at a signal to noise ratio of 3 have been calculated and they are 0.42 mM, 88, and 76 μM respectively. In LOD results too MWCNTs-PBCB possesses lower LOD than at other two modified GCEs. The overall view of these results reveals that MWCNTs-PBCB composite film is efficient for folic acid analysis.

DPV and selectivity studies of folic acid at MWCNTs-PBCB composite film.—Figure 7 shows the differential pulse voltammograms recorded for the addition of different folic acid concentrations at MWCNTs-PBCB composite film modified GCE present in PBS. After each successive folic acid addition pre-purified N_2 gas was purged into PBS for 1 min before starting the next differential pulse voltammogram. From the corresponding differential pulse voltammograms the Ipc values are plotted against folic acid concentrations as shown in Fig. 7 inset. From this inset plot it is obvious that MWCNTs-PBCB composite film exhibit a steady state response towards the addition of various folic acid concentrations, and the reduction peak current increases linearly from 0.9 to 2.31 mM folic acid. From the slopes of linear calibration curve the sensitivity and the correlation coefficient of MWCNTs-PBCB composite film have been calculated and they are 72.2 μA mM^{-1} cm^{-2} and 0.9947 respectively. Similarly, folic acid's LOD at MWCNTs-PBCB composite film at a signal to noise ratio of 3 is 96 μM. In general DPV results reveal that MWCNTs-PBCB composite film is more efficient for folic acid determination. The comparison of MWCNTs-PBCB composite film modified GCE with that of previously reported electrodes (Table II) reveals MWCNTs-PBCB possesses two advantages as follows; (1) the detection of folic acid can be carried out in neutral *p*H using MWCNTs-PBCB and (2) lower in over potential of folic acid at MWCNTs-PBCB. However some of the electrodes show better detection limit.

The DPV experiments for selectivity studies have been carried out using various analytes such as ascorbic acid, acetic acid, uric acid and dopamine. In selectivity experiments the concentration of folic acid was kept constant at 1 mM, and then each analyte was added at 50 μM. The interference of the analytes during folic acid determination has been calculated from the variation between Ipc values of folic acid before and after the addition of analytes. Where, the interference of ascorbic acid is –3.0 μA mM^{-1}, acetic acid is –7.0 μA mM^{-1}, uric acid is –7.0 μA mM^{-1} and dopamine is –0.5 μA mM^{-1}. The results show also the presence of analytes decreases the Ipc of folic acid. These above selectivity experimental results reveal

Table II. Comparison of electroanalytical results for folic acid (oxidation/reduction) at various modified electrodes in various conditions.

Electrodes	Method	*p*H	Epa/Epc (mV)	Linear range (mM)	LOD (μM)	Refs.
MWCNTs-PBCB	DPV	7.0	–560	0.9 – 2.31	96	Present work
Polymer-immobilized sol-gel PGE	DPCSV	2.5	–580	0.02 – 0.3	0.005	1
p-AMT	i–t curve	7.2	900	0.0001–0.8	0.0002	6
PMo_{12}-PPy	DPV	<3	100	0.00001–0.0001	0.0001	7
Ni/POA/CPE	CV	13	600	0.1–5.0	91	41
SWCNTs	CV	5.5	–700	0.00001–0.1	0.001	42
MWCNTs	Stripping voltammetry	6.4	–650	0.0003–0.08	0.13	43

Table III. Electroanalytical values obtained from the vitamin B_9 tablet's determination using DPV in PBS at MWCNTs-PBCB composite film modified GCE.

Added (mM)	Found (mM)	Recovery (%)	RSD (%)
0.96	0.91	95	1.1
1.75	1.64	93	—
2.42	2.25	93	—

that MWCNTs–PBCB composite film can be used for folic acid determination in real samples.

Analysis of vitamin B_9 tablet.—The performance of MWCNTs-PBCB composite film modified GCE has been tested by applying it to the determination of folic acid present in vitamin B_9 tablet. The technique used for the determination was DPV, and the experimental conditions were similar to that of DPV studies given in the above section. The vitamin B_9 tablets were obtained from a Taiwan's pharmaceutical company. The tablet's labeled composition is 5 mg of folic acid. The concentrations added in the experiment, found and relative standard deviation (RSD) obtained from the experiments are given in Table III. From the results given in Table III the recovery of folic acid was ≈ 94%, based on the assumption that the composition was exactly 5 mg, as per the manufacturer. These above results show that MWCNTs-PBCB composite film is efficient for folic acid determination.

Conclusions

Composite material containing MWCNTs and PBCB at GCE has been reported. The developed MWCNTs-PBCB composite film for the electrocatalysis combines the advantages of ease of fabrication, high reproducibility and sufficient stability. The SEM and AFM results have shown the difference between PBCB and MWCNTs-PBCB composite film's morphology. Further, it has been found that MWCNTs-PBCB composite film has an excellent functional property along with good electrocatalytic activity on folic acid. The experimental methods of CV and DPV with MWCNTs-PBCB composite film presented in this article provide an opportunity for qualitative and quantitative characterization of vitamin B_9 voltammetric sensor.

Acknowledgment

This work was supported by the National Science Council and the Ministry of Education of Taiwan (Republic of China).

National Taipei University of Technology assisted in meeting the publication costs of this article.

References

1. B. B. Prasad, R. Madhuri, M. P. Tiwari, and P. S. Sharma, *Sens. Actuators B*, **146**, 321 (2010).
2. S. Wei, F. Zhao, Z. Xu, and B. Zeng, *Microchim. Acta*, **152**, 285 (2006).
3. R. M. A. Von Wandruzska and R. J. Hurtubise, *Anal. Chim. Acta*, **93**, 331 (1977).
4. R. H. F. Chenug, P. D. Morrison, D. M. Small, and P. J. Marriott, *J. Chromatogr. A*, **1213**, 93 (2008).
5. G. R. Rao, G. Kanjilal, and K. R. Mohan, *Analyst* (Cambridge, U.K.), **103**, 993 (1978).
6. P. Kalimuthu and S. A. John, *Biosens. Bioelectron.*, **24**, 3575 (2009).
7. H. X. Guo, Y. Q. Li, L. F. Fan, X. Q. Wu, and M. D. Guo, *Electrochim. Acta*, **51**, 6230 (2006).
8. U. Yogeswaran and S. M. Chen, *Sens. Actuators B*, **130**, 739 (2008).
9. C. P. McMahon, G. Rocchitta, S. M. Kirwan, S. J. Killoran, P. A. Serra, J. P. Lowry, and R. D. O'Neill, *Biosens. Bioelectron.*, **22**, 1466 (2007).
10. H. A. Al Attar and A. P. Monkman, *J. Phys. Chem. B*, **111**, 12418 (2007).
11. K. Pu and B. Liu, *Biosens. Bioelectron.*, **24**, 1067 (2009).
12. I. Becerik and F. Kadirgan, *Synth. Met.*, **124**, 379 (2001).
13. T. Selvaraju and R. R. Ramaraj, *J. Electroanal. Chem.*, **585**, 290 (2005).
14. M. Mao, D. Zhang, T. Sotomura, K. Nakatsu, N. Koshiba, and T. Ohsaka, *Electrochim. Acta*, **48**, 1015 (2003).
15. M. Yasuzawa and A. Kunugi, *Electrochem. Commun.*, **1**, 459 (1999).
16. C. P. Andrieux, O. Haas, and J. M. SavGant, *J. Am. Chem. Soc.*, **108**, 8175 (1986).
17. J. Wang and M. Musameh, *Anal. Chim. Acta*, **511**, 33 (2004).
18. H. Cai, X. Cao, Y. Jiang, P. He, and Y. Fang, *Anal. Bioanal. Chem.*, **375**, 287 (2003).
19. A. Erdem, P. Papakonstantinou, and H. Murphy, *Anal. Chem.*, **78**, 6656 (2006).
20. H. Beitollahi, M. M. Ardakani, H. Naeimi, and B. Ganjipour, *J. Solid State Electrochem.*, **13**, 353 (2009).
21. Q. Li, J. Zhang, H. Yan, M. He, and Z. Liu, *Carbon*, **42**, 287 (2004).
22. J. Zhang, J. K. Lee, Y. Wu, and R. W. Murray, *Nano Lett.*, **3**, 403 (2003).
23. C. Deng, J. Chen, M. Wang, C. Xiao, Z. Nie, and S. Yao, *Biosens. Bioelectron.*, **24**, 2091 (2009).
24. R. J. Chen, Y. Zhang, D. Wang, and H. Dai, *J. Am. Chem. Soc.*, **123**, 3838 (2001).
25. Y. Umasankar, A. P. Periasamy, and S. M. Chen, *Talanta*, **80**, 1094 (2010).
26. A. A. Karyakin, E. E. Karyakina, and H. L. Schmidt, *Electroanalysis*, **11**, 149 (1999).
27. A. G. MacDiarmid, J. C. Chiang, A. G. Richter, and A. Epstein, *Synth. Met.*, **18**, 285 (1987).
28. R. Mazeikiene, G. Niaura, O. Eicher-Lorka, and A. Malinauskas, *Vib. Spectrosc.*, **47**, 105 (2008).
29. D. W. Yang and H. H. Liu, *Biosens. Bioelectron.*, **25**, 733 (2009).
30. A. Balamurugan and S. M. Chen, *J. Solid State Electrochem.*, **14**, 35 (2010).
31. M. E. Ghica and C. M. A. Brett, *J. Electroanal. Chem.*, **629**, 35 (2009).
32. H. Su, R. Yuan, Y. Chai, Y. Zhuo, C. Hong, Z. Liu, and X. Yang, *Electrochim. Acta*, **54**, 4149 (2009).
33. D. R. S. Jeykumari and S. S. Narayanan, *Biosens. Bioelectron.*, **23**, 1404 (2008).
34. G. M. Morris, D. S. Goodsell, R. S. Halliday, R. Huey, W. E. Hart, R. K. Belew, and A. J. Olson, *J. Comput. Chem.*, **19**, 1639 (1998).
35. J. Fuhrmann, A. Rurainski, H.-P. Lenhof, and D. Neumann, *J. Comput. Chem.*, **31**, 1911 (2010).
36. M. D. Rubianes and G. A. Rivas, *Electrochem. Commun.*, **9**, 480 (2007).
37. U. Yogeswaran and S.-M. Chen, *J. Electrochem. Soc.*, **154**, E178 (2007).
38. K.M. Shin, J. Lee, G. G. Wallace, and S. J. Kim, *Sens. Actuators B*, **133**, 393 (2008).
39. A. Mohadesi and M. A. Taher, *Sens. Actuators B*, **123**, 733 (2007).
40. J. Wang, J. Dai, and T. Yarlagadda, *Langmuir*, **21**, 9 (2005).
41. R. Ojani, J. B. Raoof, and S. Zamani, *Electroanalysis*, **21**, 2634 (2009).
42. C. Wang, C. Li, L. Ting, X. Xu, and C. Wang, *Microchim. Acta*, **152**, 233 (2006).
43. X. L. Jiang, R. Li, J. Li, and X. He, *Russ. J. Electrochem.*, **45**, 772 (2009).